Lifetime measurements of cesium $5d\ ^2D_{5/2,3/2}$ and $11s\ ^2S_{1/2}$ states using pulsed-laser excitation

D. DiBerardino* and C. E. Tanner
Department of Physics, University of Notre Dame, Notre Dame, Indiana 46556

A. Sieradzan
Department of Physics, Central Michigan University, Mount Pleasant, Michigan 48859

(Received 18 December 1997)

We report measurements of the $5d\ ^2D_{5/2}$, $5d\ ^2D_{3/2}$, and $11s\ ^2S_{1/2}$ state lifetimes in the ^{133}Cs atom to be 1281(9), 909(15), and 351(4) ns, respectively. A pulsed-dye laser selectively excites atomic Cs from the ground state, via a single-photon quadrupole transition, to the $5d$ states and, via a two-photon electric dipole transition, to the $11s$ state. A spectrometer-photomultiplier system detects the fluorescence from the decay of interest and a digitizing oscilloscope records the direct output of the photomultiplier. The data are fit to an exponential function to yield a value for the mean lifetime of the selected state. [S1050-2947(98)01106-8]

PACS number(s): 32.70.Cs,42.55.Mv,42.62.Fi

INTRODUCTION

Measurements of atomic lifetimes are important in many areas of physics, including astrophysics, geophysics, and plasma physics. Scientists in these fields use the values of oscillator strengths to determine relative abundances of elements. Accurate atomic lifetimes are needed to calculate absolute values of oscillator strengths. Lifetime measurements also play the important role of evaluating the accuracy of atomic structure calculations. In particular, radial matrix elements between low-lying states in atomic cesium are used to test the theory necessary for interpretation of parity nonconserving (PNC) effects. Alkali-like atoms, with a single electron outside a closed shell, provide the simplest open shell systems for detailed comparison between experiment and theory.

Recent lifetime measurements in cesium are motivated by a precise measurement of PNC by Wood *et al.* [1]. Our group measured, using laser excitation of a fast atomic beam, the $6p\ ^2P_{3/2,1/2}$ state lifetimes and obtained precisions better than 0.30% [2]. Additionally, Young *et al.* [3] have measured, using pulsed-laser time-resolved spectroscopy, the $6p\ ^2P_{3/2,1/2}$ state lifetimes with similar precision. More recently, Hoeling *et al.* [4] have measured, using pulsed-laser time-resolved spectroscopy, the $5d\ ^2D_{5/2}$ state lifetime to a precision of 1%. We began our investigation of the $5d\ ^2D$ states because of a discrepancy between theory [5] and the experiment of Hoeling *et al.* [4]. We improve upon the precision of [4] and include the $5d\ ^2D_{3/2}$ state as well as the $11s\ ^2S_{1/2}$ state.

SETUP

A Nd^{3+}:YAG (YAG denotes yttrium aluminum garnet) laser pumps a dye laser to produce 8 ns pulses with 6 mJ of energy at the interaction region at a repetition rate of 10 Hz. At these intensities, populations produced in excited states are a small fraction of the total number of atoms. A digital delay and pulse generator fires the Q switch at nonoptimal delays to reduce the laser intensity and provide the trigger electronics. The linewidth of the laser, 0.10 cm^{-1}, exceeds the Fourier transform limited value and is narrow enough to selectively excite cesium from either the $F=3$ or $F=4$ $6s\ ^2S_{1/2}$ ground state hyperfine levels separated by 9.19 GHz. As shown in Fig. 1 the output from the dye laser travels through an aperture to reduce scattered light, then through a beam-shaping lens before reaching the 2.5 cm diameter Cs cell. The large size of the cell allows us to ignore wall collision effects since they should be negligible for this geometry. Scattered light is not a problem since the photomultiplier tube (PMT) always detects at a wavelength different from that of the excitation process. The cell is kept at room temperature, 293 K, giving a Cs density of 3×10^{10} atoms/cm^3. For such a low density, collisional effects such as atom-atom interactions, collisional ionization, and collisional mixing are negligible. Helmholtz coils surround the interaction region, reducing stray fields to less than 5 mG, thus eliminating the problem of Zeeman beats. For the $5d\ ^2D$ state lifetime measurements quantum beats between hyperfine states are not a concern since we view the $6p\ ^2P$ decays and any beats are on the order of a couple hundred

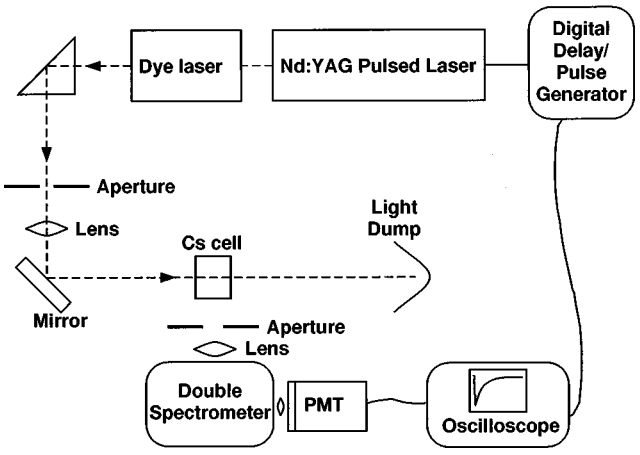

FIG. 1. Schematic of the setup.

*Electronic address: ddiberar@pesto.phys.nd.edu

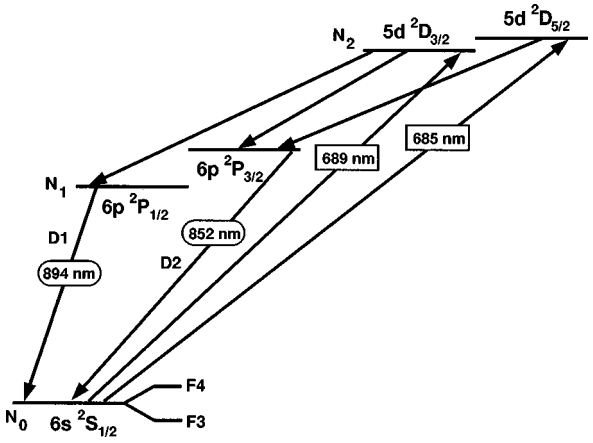

FIG. 2. Energy-level diagram showing the states of interest used for measuring the $5d\ ^2D$ lifetimes.

MHz. For the $11s\ ^2S_{1/2}$ state lifetime measurement, hyperfine quantum beats are not present in our detection scheme since we view the fluorescence from the $11s\ ^2S$ state and the gyromagnetic factors for the two F levels are equal and opposite. The size of the interaction region is determined by the size of the laser beam, about 1 cm long by 2 mm wide, and the solid angle of the collection optics.

After a pulse excitation, fluorescent photons impinge upon a collimating lens before entering the spectrometer for wavelength selection. A red-sensitive PMT sits at the output of the spectrometer. Since we view the $6p\ ^2P \rightarrow 6s\ ^2S$ transition photons at wavelengths of 852 nm and 894 nm, we must use a PMT with a low work function GaAs:Cs-O photocathode that detects longer wavelength photons. The electronics setup is simplified by integrating the PMT signal directly with a 1 GHz digitizing oscilloscope, eliminating any ringing effects from extra components. Because we do not discriminate the PMT signal, the background in a typical run includes dark counts on the order of 20 per second. At time $t=0$, the laser is pulsed off and the oscilloscope records into 1024 channels the current of the PMT, terminated with 50 Ω, as a function of time with a full time scale approximately equal to ten decay lengths. This is repeated for either 16 384 or 8192 cycles as the data are averaged after each cycle. We convert the oscilloscope voltage signal to a photon-counting signal with the factor,

$$(\text{factor}) = \frac{T_{\text{tot}}(\text{number of averages})}{(\text{number of channels})(\Omega)(q)(\text{PMT gain})}, \tag{1}$$

where T_{tot} is the full time scale of the oscilloscope; the number of averages is 16 384 or 8192; $\Omega = 50\ \Omega$, the oscilloscope input impedance; $q = -1.6\times10^{-19}$ C, the charge of one electron; the number of channels is 1024; and PMT gain is 5×10^5. With this conversion, the standard deviation in the voltage is consistent with the square root of the number of photon counts, demonstrating that we are operating in a regime that is limited by photon-counting statistics.

$5d\ ^2D_{5/2,3/2}$ states

Figure 2 shows the energy level diagram with the states of interest. In general, let N_0 be the ground state population, N_2 the population of the excited state of interest, N_{1a} the population of the $6p\ ^2P_{3/2}$ state, and N_{1b} the population of the $6p\ ^2P_{1/2}$ state. Then, we can call τ_2 the lifetime of the state of interest, τ_{1a} the $6p\ ^2P_{3/2}$ lifetime, and τ_{1b} the $6p\ ^2P_{1/2}$ lifetime.

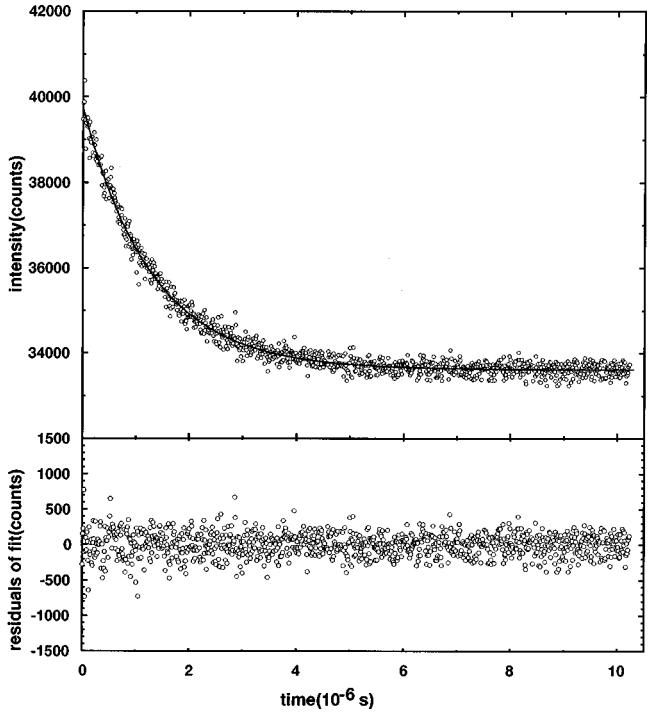

FIG. 3. Typical decay curve of $5d\ ^2D_{5/2}$ state with fitting function and residuals.

For the $5d\ ^2D_{5/2}$ measurement, the dye laser is tuned to the electric quadrupole ($E2$) transition, $6s\ ^2S_{1/2} \rightarrow 5d\ ^2D_{5/2}$, at a wavelength of 685 nm with an oscillator strength of 6×10^{-7} [6]. The excited state decays with a lifetime τ_2 to the $6p\ ^2P_{3/2}$ state, that then decays with a lifetime τ_{1a} to the ground state, releasing a photon of wavelength 852 nm. For the $5d\ ^2D_{3/2}$ measurement, the dye laser is tuned to the $E2$ transition, $6s\ ^2S_{1/2} \rightarrow 5d\ ^2D_{3/2}$, at a wavelength of 689 nm with an oscillator strength of 3×10^{-7} [6]. The $5d\ ^2D_{3/2}$ state decays with a lifetime τ_2 to either $6p\ ^2P$ state. The spontaneous transition probabilities for these processes may be determined from Ref. [7] as

$$A(5d\ ^2D_{3/2} \rightarrow 6p\ ^2P_{3/2}) = 9.7\times10^4\ \text{s}^{-1}, \tag{2}$$

$$A(5d\ ^2D_{3/2} \rightarrow 6p\ ^2P_{1/2}) = 8.4\times10^5\ \text{s}^{-1}. \tag{3}$$

A cesium atom in either the $6p\ ^2P_{3/2}$ state or the $6p\ ^2P_{1/2}$ state decays to the ground state, releasing photons of wavelengths 852 nm and 894 nm, respectively.

The spectrometer is tuned to the wavelength of interest and the PMT detects this fluorescence. The signal is sent to the oscilloscope to give a typical curve as shown in Fig. 3. This fluorescence spectrum is proportional to the population, N_{1a} or N_{1b}, of the upper state from which it comes. When the laser is turned off, the populations are given by

$$N_{1a}(t)=\frac{\tau_2\tau_{1a}}{\tau_2-\tau_{1a}}A_{2,1a}N_2(0)\times\left\{\left(\frac{N_{1a}(0)}{N_2(0)}\frac{\tau_2-\tau_{1a}}{A_{2,1a}\tau_2\tau_{1a}}-1\right)e^{-t/\tau_{1a}}+e^{-t/\tau_2}\right\}, \tag{4}$$

$$N_{1b}(t)=\frac{\tau_2\tau_{1b}}{\tau_2-\tau_{1b}}A_{2,1b}N_2(0)\times\left\{\left(\frac{N_{1b}(0)}{N_2(0)}\frac{\tau_2-\tau_{1b}}{A_{2,1b}\tau_2\tau_{1b}}-1\right)e^{-t/\tau_{1b}}+e^{-t/\tau_2}\right\}. \tag{5}$$

In these equations, $A_{2,1a}$ and $A_{2,1b}$ are the spontaneous transition probabilities for decay to the $6p\ ^2P_{3/2}$ state and the $6p\ ^2P_{1/2}$ state, respectively, and $N_2(0)$ and $N_{1a,b}(0)$ are the state populations at $t=0$. Specifically, the $5d\ ^2D_{5/2}$ state decays solely to the $6p\ ^2P_{3/2}$ state with $A_{2,1a}=7.0\times10^5\ \mathrm{s}^{-1}$ [7] and $A_{2,1b}=0$. On the other hand, the $5d\ ^2D_{3/2}$ state decays to either $6p$ state with $A_{2,1a}$ and $A_{2,1b}$ given in Eq. (2) and Eq. (3), respectively. After a sufficient time $t\gg\tau_{1a,b}$, the first term in these equations will become much smaller than the second term. For example, at $t=700$ ns the first term ($e^{-t/\tau_{1a,b}}$) is less than 10^{-11} times smaller than the second term (e^{-t/τ_2}). Therefore we delay the recording of the data by 700 ns from $t=0$ and fit the curve to a single exponential given by the second term in both Eq. (4) and Eq. (5). In addition, this ensures that PMT saturation, which can occur near $t=0$, is negligible.

$11s\ ^2S_{1/2}$ state

Figure 4 shows the energy levels of interest in this setup. As before, N_0 is the ground state population and N_2 is the population of the excited state of interest. The dye laser, tuned to a wavelength of 687 nm, excites the Cs atoms via a two-photon electric dipole ($E1$) transition from the ground state to the $11s\ ^2S_{1/2}$ state. This state decays with a lifetime τ_2 to either the $6p\ ^2P_{3/2}$ or the $6p\ ^2P_{1/2}$ state, emitting photons of wavelengths 575 nm and 557 nm, respectively. The spontaneous transition probabilities are found in Ref. [7]:

$$A(11s\ ^2S_{1/2}\rightarrow6p\ ^2P_{1/2})=4.0\times10^5\ \mathrm{s}^{-1}, \tag{6}$$

$$A(11s\ ^2S_{1/2}\rightarrow6p\ ^2P_{3/2})=6.0\times10^5\ \mathrm{s}^{-1}. \tag{7}$$

Since both direct decays to the $6p\ ^2P$ states are observable with our PMT, we can detect either fluorescence from the state of interest, giving a curve which is governed by a single exponential. This spectrum should be proportional to the population, N_2, of the $11s\ ^2S_{1/2}$ state and given by the general form

$$N_2(t)=N_2(0)e^{-t/\tau_2}. \tag{8}$$

We did not delay the recording of these data since radiation trapping is not a concern. However, we did check for PMT saturation, as shown in our analysis.

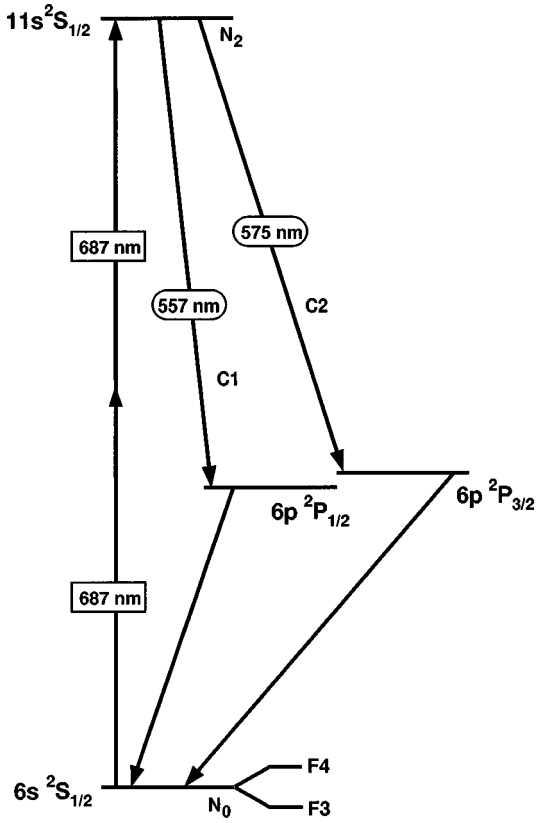

FIG. 4. Energy-level diagram showing the states of interest for measuring the $11s\ ^2S_{1/2}$ lifetime.

ANALYSIS

Since the laser can resolve the ground state hyperfine splitting, we utilize the two excitation routes from the $F=3$ and $F=4$ $6s\ ^2S_{1/2}$ states to the upper level. Additionally, there is usually more than one decay route producing photons that are in the range of the PMT. A decay from $6p\ ^2P_{3/2}\rightarrow6s\ ^2S_{1/2}$ is a $D2$ transition and a decay from $6p\ ^2P_{1/2}\rightarrow6s\ ^2S_{1/2}$ is a $D1$ transition. We refer to any decay to the $6p\ ^2P_{3/2}$ state as a $C2$ decay and any decay to the $6p\ ^2P_{1/2}$ state as a $C1$ decay. Therefore we describe any experimental scheme by the notation (excitation route, fluorescence monitor), where $F3$ or $F4$ is the excitation route and $D1$, $D2$, $C1$, or $C2$ is the fluorescence monitor. Initially, the fitting program truncates the data at regular increments, thus enabling us to look for any systematic effects that change with time such as scattered light, radiation trapping, and PMT saturation. A nonlinear least-squares routine developed by Levenberg and Marquardt [8] fits each data file to an exponential function.

There are several laser-intensity effects which can alter the measured lifetimes. These include multiphoton ionization, molecular excitation, glass cell fluorescence, and atomic excitation by an amplified spontaneous emission (ASE) component in the laser light. We expect that molecular excitations are negligible in this setup since the cell is kept at room temperature. Also, multiphoton ionization is dependent upon the third power of the laser intensity, and at intensities used in this experiment this effect should be small. Similarly, there is no indication that the PMT observes fluorescence from the glass cell. However, ASE-related con-

tributions should be considered in these precision lifetime measurements. The ASE spectrum has a power versus wavelength distribution similar to the dye amplification curve. This distribution extends from 645 nm to 730 nm with a maximum at 690 nm. The total power in the distribution is about 1% of the dye laser output power. When the ASE from the dye excites a cesium atom, the absorption spectrum of the transition determines the width of the transition and thus the percentage of the power imparted to that excitation. ASE is a problem in the $5d\ ^2D$ setup for a couple of reasons. First, the laser is tuned to an electric quadrupole transition which is much weaker than an ASE-induced electric dipole transition. Second, the PMT detects photons from the $6p\ ^2P$ states that decay to the ground state. Most undesired cascades decay through these states, producing unwanted photons. For example, the laser, tuned to the $6s\ ^2S_{1/2}\rightarrow 5d\ ^2D$ transition, may excite an atom, via an $E1$-allowed process, to an intermediate virtual p state. Then, an ASE photon at a wavelength 645 nm$<\lambda_{\mathrm{ASE}}<$730 nm may excite, via an $E1$-allowed process, this atom to some even-numbered angular momentum state. These states then decay through a multitude of routes. Alternatively, an ASE photon at λ_{ASE} may excite an atom already in the $5d\ ^2D$ state to an odd-numbered angular momentum state that then decays through some path to the ground state. All of these cascades enter into the rate equations and thus show up as additional terms in Eq. (4) and Eq. (5). Each term depends on the lifetime of some upper state, the population of that upper state, and the spontaneous transition probability of observing a decay from that upper state to some lower state.

We observe these ASE effects directly when measuring the $5d\ ^2D_{3/2}$ lifetime. The PMT views both the $6p\ ^2P_{3/2}$ decay and the $6p\ ^2P_{1/2}$ decay. A discrepancy in the observed lifetimes for these two decay routes results since the unwanted cascades influence these populations in different proportions. Furthermore, this effect can also influence the observed lifetime of the $5d\ ^2D_{5/2}$ state. We have no direct observation of the ASE effect on this lifetime, but we can estimate how large the effect is. In contrast, ASE should have no impact on the measured $11s\ ^2S_{1/2}$ lifetime since the PMT detects the photons that decay directly from the $11s$ state and the laser excites the atom into a highly excited state.

$5d\ ^2D_{5/2}$ results

There are ten runs using a $(F4,D2)$ scheme and ten runs using a $(F3,D2)$ scheme (see Fig. 2). For a single run data are truncated in 200 ns increments to give us 16 files to fit to a function of the form

$$y(t)=Ae^{-t/\tau_2}+B, \tag{9}$$

where A is the amplitude of the curve, B is the background, and τ_2 is the mean lifetime of the state. A graph of the value τ_2 versus truncation for one run is shown in Fig. 5. As we cut the data, the fitting routine has increasing difficulty pinpointing the parameter B.

This creates a shift in the lifetime with truncation. To determine the background and its uncertainty we use three methods; each can be compared with the others. First, the tail of the data gives an estimate of B and its corresponding

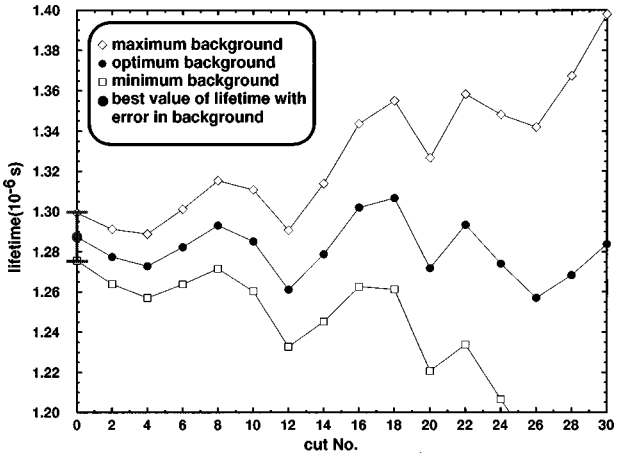

FIG. 5. Lifetime versus truncation for a typical $5d\ ^2D_{5/2}$ data run. The three graphs represent three possible values for the background.

statistical uncertainty. Also, if B floats when the program fits the untruncated data, this gives a second estimate of the background. Lastly, we determine the background to be that value of B which gives a lifetime that is most stable against truncations and is in fair agreement with the other two. From the spread in these estimates of B, we can assign an uncertainty to τ_2 due to the uncertainty in the background.

Having determined B, we use a plot such as Fig. 5 for each run to check for systematic shifts in the lifetime as a function of truncation that might be indicative of saturation, radiation trapping, or quantum beats. If there are no apparent shifts we take the untruncated value of τ_2 with an uncertainty given by the sum in quadrature of the background uncertainty and the statistical uncertainty with no truncations. In Fig. 5 the large black circle is the lifetime value found for this particular run, where the error bar is due to background uncertainty alone. If there is a truncation dependent shift, we take the value of τ_2 at the truncation where the trend becomes less than the statistical uncertainty. Again, the overall uncertainty in the run is the sum in quadrature of the statistical uncertainty and the background uncertainty at that truncation. The average uncertainty due to statistics and background is given by the weighted mean of the uncertainties in each run.

To check for ASE plus virtual p state effects and ionization, the monochromator is set to transmit light from a $9d\ ^2D\rightarrow 6p\ ^2P$ transition, and the detection system acquires data as in a typical run. The observed fluorescence is less than 1.0(5)% of the $6p\ ^2P_{3/2}$ signal amplitude. We calculate the effect that this cascade could have on our lifetime evaluation and find a shift of $+2(1)$ ns. The uncertainty given is the sum in quadrature of the uncertainty in the signal amplitude plus the uncertainty in the lifetimes of these unwanted states. Similarly, using this same spectrum we place an upper bound on ionization effects to be ± 2 ns.

To check for ASE plus excited d state effects, the digital delay fires the Q switch at an optimal delay to give a maximum laser intensity. We tune the spectrometer to the $D1$ line while the laser excites Cs atoms to the $5d\ ^2D_{5/2}$ level and the oscilloscope acquires data as it would for a lifetime run. This spectrum contains cascades through the $6p\ ^2P_{1/2}$ state that may arise from ionization or ASE-induced effects. The am-

TABLE I. Summary of all uncertainties and shifts for each state.

State of interest	$5d\ ^2D_{3/2}$		$5d\ ^2D_{5/2}$	$11s\ ^2S_{1/2}$
Decay route viewed	$D1$	$D2$	$D2$	$C1,C2$
Mean result[a]	925 ns	995 ns	1288 ns	351 ns
Statistics plus background	± 4 ns	± 5 ns	± 4 ns	± 2 ns
Ionization	± 2 ns	± 4 ns	± 2 ns	± 3 ns
ASE plus virtual p state	$+2\pm 1$ ns	$+8\pm 4$ ns	$+2\pm 1$ ns	
ASE plus excited d state	-18 ± 14 ns	-91 ± 87 ns	-9 ± 8 ns	
Other[b]	± 0.5 ns	± 0.5 ns	± 0.5 ns	± 0.5 ns
Total	909(15) ns	912(87) ns	1281(9) ns	351(4) ns

[a]Weighted by statistics plus background.

[b]Includes quantum beats, atom-atom and wall collisions, radiation trapping, and blackbody radiation.

plitude of this signal is below 0.5(2)% of the on-resonance $6p\ ^2P_{3/2}$ signal. Since the PMT is about five times more sensitive at a wavelength of 852 nm than it is at 894 nm, the actual percentage of the $6p\ ^2P_{3/2}$ signal due to these cascades is closer to 3(1)%. Furthermore, when the laser is detuned from the $5d\ ^2D_{5/2}$ level about half of the signal, 1.5(5)%, from the $6p\ ^2P_{1/2}$ state remains. In this situation there is no ASE-induced resonance; thus there is a reduction in the signal size. Next, we detune the laser and set the monochromator to transmit the off-resonant $6p\ ^2P_{3/2}$ signal. The signal is about 0.5(2)% of the on-resonant $6p\ ^2P_{3/2}$ signal. We assume that the $D2$ on-resonance contribution is about a factor of 2 larger than the $D2$ off-resonance contribution, as was shown in the $D1$ signal, and we get a final value of 1.0(4)%. This 1.0(4)% signal amplitude comprises both ionization and ASE-induced resonance effects. Our collective estimate for ASE-induced resonance effects is 0.5(3)% of the on-resonant signal. During an actual data run the digital delay fires the Q switch at nonoptimal delays as a means for adjusting the laser intensity. The typical laser intensity is approximately 20% of the maximum laser intensity used in these tests. The fractional size of ASE effects is larger by a factor of 5 at this lower laser intensity and ionization effects are reduced by a factor of 125. Thus we estimate that the ASE-induced resonance effects contribute 3(2)% to the $6p\ ^2P_{3/2}$ signal amplitude, corresponding to a $-9(8)$ ns shift in the lifetime. The error in the shift is the sum in quadrature of the uncertainty in the amplitude plus the uncertainty in the lifetimes of these unwanted states.

Other systematic effects include quantum beats, atom-atom collisions, wall collisions, blackbody radiation, and radiation trapping. These effects contribute less than ± 0.5 ns to the uncertainty in the measured lifetime. We take the weighted mean of the lifetimes from the 20 runs using the statistical plus background uncertainties and include the systematic shifts in the measured lifetime. We obtain a $5d\ ^2D_{5/2}$ lifetime of 1281(9) ns, where the error is the sum in quadrature of the errors due to background fluctuations plus statistics, laser-intensity effects, and other systematic effects. A summary of these uncertainties and shifts is shown in Table I. Figure 6 is a plot of the 20 runs with individual error bars from background fluctuations and statistics given. We show our final result in Fig. 7 and compare it to other experiments and theory.

$5d\ ^2D_{3/2}$ results

There are eight runs using a $(F4,D2)$ scheme, eight runs using a $(F3,D2)$ scheme, eight runs using a $(F3,D1)$ scheme, and eight runs using a $(F4,D1)$ scheme. For a single run we truncate the data in 200 ns increments, obtaining 16 files. If we fit both the $D1$-viewed data and the $D2$-viewed data to a function of the form in Eq. (9) and

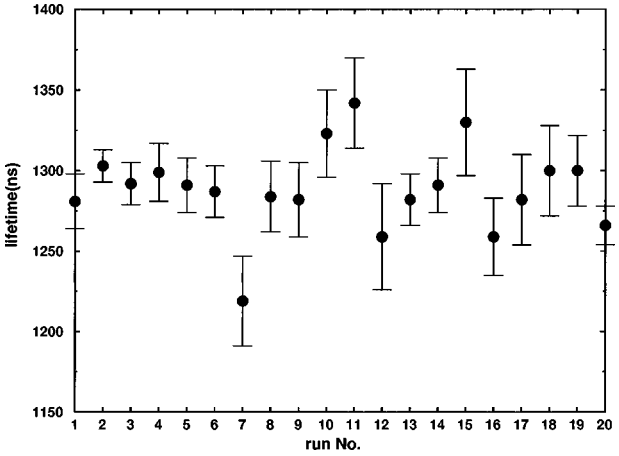

FIG. 6. All $5d\ ^2D_{5/2}$ runs with error bars given by the sum in quadrature of the statistical uncertainty plus background uncertainty.

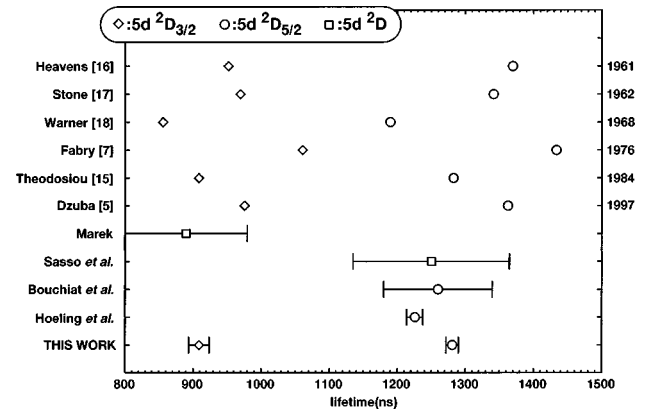

FIG. 7. Survey of $5d\ ^2D$ lifetime measurements. Theoretical values are plotted without error bars. Experimental values are plotted with error bars.

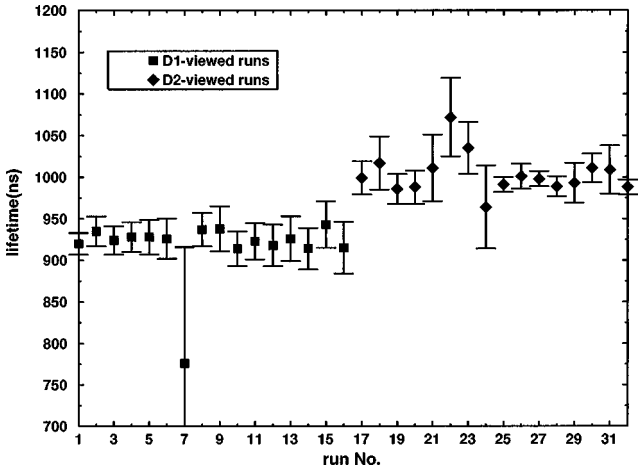

FIG. 8. All $5d\ ^2D_{3/2}$ runs with error bars given by the sum in quadrature of the statistical uncertainty plus background uncertainty. Apparent is an offset in the fitted value of the lifetime due to ASE-induced effects.

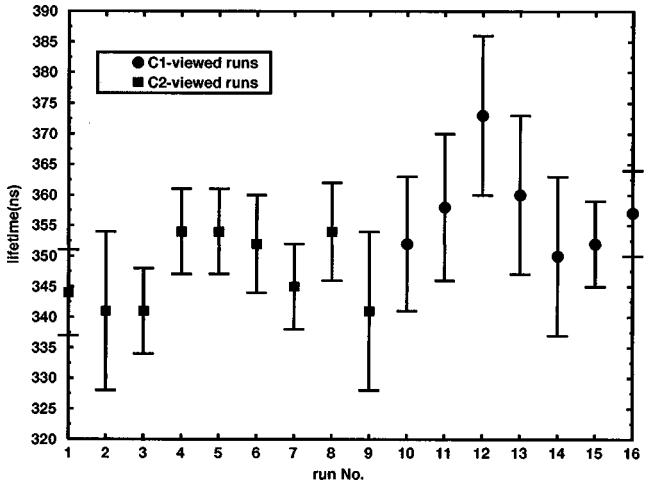

FIG. 9. All $11s\ ^2S_{1/2}$ runs with error bars given by the sum in quadrature of the statistical uncertainty plus background uncertainty.

proceed as we did in the $5d\ ^2D_{5/2}$ analysis we obtain different values for the lifetime: $\tau_2(D1\ \text{view})=925(4)$ ns and $\tau_2(D2\ \text{view}) = 995(5)$ ns, where the error is just the statistical uncertainty summed in quadrature with the background uncertainty (see Fig. 8). This discrepancy is an indication that either ionization, ASE effects, or both are contributing to the signal and shifting fitted values of the lifetimes. Since the spontaneous transition probabilities given in Eq. (2) and Eq. (3) indicate that the $5d\ ^2D_{3/2}$ state decays almost exclusively to the $6p\ ^2P_{1/2}$ state, it is reasonable to assume that ionization and ASE effects have a greater impact on the $D2$-viewed lifetime.

To determine the size of the ASE plus excited d state contribution, the digital delay fires the Q switch at an optimal delay to give a maximum laser intensity. Then, we detune the laser from the $6s\ ^2S_{1/2}\rightarrow 5d\ ^2D_{3/2}$ transition while the PMT observes the chosen route. The amplitude of the off-resonant $D1$ signal is about 2.0(5)% of the amplitude of the on-resonant $D1$ signal, while the amplitude of the off-resonant $D2$ signal is about 7(2)% of the amplitude of the on-resonant $D2$ signal. In both cases, the signal size was independent of laser tuning. Nevertheless, this does not directly tell us the effect that ionization or ASE has on the signal when the laser is tuned on resonance. The $5d\ ^2D_{5/2}$ tests give us an indication. In the $5d\ ^2D_{5/2}$ case, the off-resonant effects for the $D1$-viewed signal were about half of the on-resonant effects for the $D1$-viewed signal. This ionization or ASE effect is probably similar for both $5d\ ^2D$ states. The estimates give a 4(1)% signal amplitude for on-resonant $D1$-viewed data and a 14(4)% signal amplitude for on-resonant $D2$-viewed data for $5d\ ^2D_{3/2}$ excitation. In addition, at these high laser intensities ionization effects are enhanced. Ionization contributes about twice as much to the $6p\ ^2P_{3/2}$ decay as it does to the $6p\ ^2P_{1/2}$ decay. Also, ionization should account for about 50% of the on-resonant $D1$-viewed amplitude due to all laser-intensity effects. Because of this, the best estimates of the on-resonant ASE-induced amplitudes are 2(1)% for the $D1$ view and 9(6)% for the $D2$ view. The laser intensity is a maximum when the tests were performed and the laser intensity during data runs is about one-fourth of this maximum intensity. Thus there is an additional factor of 4 which multiplies these estimates to give an 8(4)% signal amplitude for on-resonant $D1$-viewed data and a 36(24)% signal amplitude for on-resonant $D2$-viewed data. We calculate the effect that these processes have on our ability to extract the desired lifetime and find a $-18(14)$ ns shift in the $D1$-observed lifetime and a $-91(87)$ ns shift in the $D2$-observed lifetime. The errors are given by the sum in quadrature of the uncertainty in the amplitude plus the uncertainty in the lifetimes of the unwanted states.

ASE plus virtual p state effects shift the $D1$-viewed lifetime by $+2(1)$ ns and the $D2$-viewed lifetime by $+8(4)$ ns. Ionization contributes a ± 2 ns error to the $D1$-viewed lifetime and a ± 4 ns error to the $D2$-viewed lifetime. These shifts are our best estimates based on the $5d\ ^2D_{5/2}$ systematic tests. We place a combined upper limit of ± 0.5 ns on other systematic effects which include quantum beats, atom-atom collisions, wall collisions, blackbody radiation, and radiation trapping.

The lifetime obtained when viewing the $D1$ transition is 909(15) ns and the lifetime obtained when viewing the $D2$ transition is 912(87) ns, where each error is the sum in quadrature of the uncertainties due to statistics plus background effects, laser-intensity effects, ionization, and other systematic effects as listed above (see Table I). The weighted mean of the $D1$-observed lifetime and the $D2$-observed lifetime gives a final value of 909(15) ns for the lifetime of the $5d\ ^2D_{3/2}$ state. Figure 7 shows this result compared with theory and previous experiments.

$11s\ ^2S_{1/2}$ results

There are nine runs using a $(F4,C2)$ scheme and seven runs using a $(F4,C1)$ scheme. For a single run data are truncated in 80 ns increments, giving us 16 files; each is fit to a function of the form in Eq. (9). These fits determine the values of τ_2 versus truncation for each run and we obtain the background as we did for the $5d\ ^2D_{5/2}$ measurement. The total uncertainty due to statistics plus background is ± 2 ns. Figure 9 shows the lifetime, given with individual statistical and background uncertainties, obtained from each run. There

TABLE II. Experimental results in comparison with other experiments and theory.

Lifetime (ns)				
$5d\ ^2D_{5/2}$	$5d\ ^2D_{3/2}$	$11s\ ^2S_{1/2}$	Method	Reference
1281(9)	909(15)	351(4)	pulsed-laser excitation	This work
1226(12)			diode-laser excitation	[4]
1260(80)			delayed probe absorption	[9]
890(90)	890(90)		delayed coincidence	[10]
1250(115)	1250(115)		time-resolved fluorescence	[11]
		343(22)	delayed-coincidence	[12]
		411(8)	time-resolved fluorescence	[13]
		403(4)	time-resolved fluorescence	[14]
1363	976		MBPT	[5]
1283	909	403	CAH[a] with core, SO[b] effects	[15]
1434	1061		CA[c] with core effects	[7]
1370	952		CA	[16]
1342	970		CA with SO effects	[17]
1190	856		Perturbation theory	[18]

[a]Coulomb approximation, Hartree potentials.
[b]Spin orbit.
[c]Coulomb approximation.

is a small difference, of about one standard deviation, between those lifetimes obtained when viewing a $C1$ decay and those lifetimes obtained when viewing a $C2$ decay. Specifically, $\tau_2(C1\ \text{view})=356(4)$ ns and $\tau_2(C2\ \text{view})= 348(3)$ ns. Such a small difference must be attributed to ionization effects which may change the fitted lifetimes determined from the two decay routes. Since the $11s\ ^2S$ state is a highly excited state, ionization is likely to occur more often than it does in the $5d\ ^2D$ measurements. Still, we view the $11s\ ^2S$ decay directly so that these effects are minimized. We estimate the uncertainty in the lifetime due to ionization to be ± 3 ns. Other systematic effects, such as atom-atom collisions, wall collisions, blackbody radiation, and radiation trapping contribute an uncertainty of ± 0.5 ns to the measured lifetime. The weighted mean of all runs gives us a lifetime of $\tau_2 = 351(4)$ ns, where the uncertainty is given by the sum in quadrature of the uncertainties due to statistics and background, ionization, and other systematic effects (see Table I).

CONCLUSIONS

Table II shows our lifetime values for the states we measured in comparison with theory and other experiments. Our work gives an $11s\ ^2S_{1/2}$ lifetime of 351(4) ns, a $5d\ ^2D_{5/2}$ lifetime of 1281(9) ns, and a $5d\ ^2D_{3/2}$ lifetime of 909(15) ns. Our values for the $5d\ ^2D$ lifetimes are in good agreement with the most recent published theoretical results of Theodosiou [15]. In Theodosiou's calculations, the atomic potential within the core (used in Schrödinger's equation) consists of three parts. Hartree potentials were used for the single-electron central field that results from the interaction between the nucleus and the core electrons. Parametric potentials given by Weisheit [20] were used to model the effects of core polarization. Lastly, the spin-orbit interaction was modeled using the full relativistic form of the potential in the Pauli approximation in which $mc^2 \gg$ (all other energies). Because the atomic core effects are represented in detail, we expect Theodosiou's results to be reliable. In Heavens's calculation [16], core polarization effects and spin-orbit effects were not included. Additionally, Stone's calculation [17] does not include core polarization effects and Fabry's calculation [7] does not include spin-orbit effects. Without inclusion of these potentials in the model, it is difficult to make a meaningful comparison with their results. In contrast, for the $11s\ ^2S$ lifetime, our result differs from Theodosiou's by $\sim 15\%$. Since the $11s\ ^2S$ state decays through numerous routes, all possible transitions must be considered in any theoretical calculation. Additionally, our $11s\ ^2S$ lifetime is in disagreement with the most recent measurement of that state by Neil and Atkinson [14]. Our setup and method are very similar to those of Neil and Atkinson [14], thus it is hard to explain this difference in experimental values.

Dzuba's preliminary *ab initio* results [5] apply relativistic many-body perturbation theory (MBPT) to calculate the electric dipole matrix elements for the $5d\ ^2D_J \rightarrow 6p\ ^2P_{J'}$ transitions. Using the relation

$$\frac{1}{\tau_J} = \sum_{J'} \frac{4}{3}\alpha \frac{\omega_{J,J'}^3}{c^2} \frac{|\langle 5D_J|r|6P_{J'}\rangle|^2}{2J+1}, \tag{10}$$

where J is the angular momentum of the upper state and J' is the angular momentum of the lower state, the theoretical lifetimes are 1363 ns for the $5d\ ^2D_{5/2}$ lifetime and 976 ns for the $5d\ ^2D_{3/2}$ lifetime. In this equation, the transition frequencies are found from [19]. His calculated $5d\ ^2D_{5/2}$ lifetime differs from our value by about 6% and his $5d\ ^2D_{3/2}$ lifetime differs from our value by about 7%. In his calculation, Dzuba includes several corrections to the zero-order value, obtained from the relativistic Hartree-Fock method. First, he takes into account the atomic core polarization due to an external electric field or the nucleus's magnetic field. Second, all second-order correlation corrections for the wave function are included. Higher-order corrections to the wave function include screening of the Coulomb interaction, hole-

particle interaction, and iterations of the self-energy operator. Calculations of the structural radiation and normalization contribution are described in some of the earlier papers of Dzuba and co-workers [21,22]. In addition, these papers provide a complete survey of all the corrections that he uses. Hoeling *et al.* report the $5d\ ^2D_{5/2}$ state lifetime to be 1226(12) ns, which is in disagreement with our result. They used an acousto-optic deflector to shutter a single-mode diode laser that is tuned to the quadrupole transition, $6s\ ^2S_{1/2} \rightarrow 5d\ ^2D_{5/2}$. Since their cell had a radius of 2 mm, wall collisions were a concern for them. They calculated that in their setup this effect should reduce the lifetime by 2.8(8)%. Additionally, there is good agreement with older experimental values of the $5d\ ^2D_{5/2}$ lifetime in cesium obtained by both Sasso *et al.* [11] and Bouchiat *et al.* [9]. Experimentally, there have been no previous direct measurements of the $5d\ ^2D_{3/2}$ lifetime. Figure 7 is a graph of these $5d\ ^2D$ values, noted in this discussion, with our results.

Note added in proof. Wo Yei, A. Sieradzan, E. Cerasuolo, and M. D. Havey published the hyperfine coupling constants of the $5d\ ^2D_j$ levels in Cs [23].

ACKNOWLEDGMENTS

We would like to acknowledge helpful discussions with H. G. Berry, A. E. Livingston, D. Current, and R. Stoleru. R. Stoleru's and D. Current's help with equipment and data analysis are appreciated. D. D. and C. E. T. would like to thank the Division of Chemical Sciences, Office of Basic Energy Sciences, Office of Energy Research at the U.S. Department of Energy for its generous support of this research under Contract No. DE-FG02-95ER14579. A. S. would like to thank the CMU Faculty Research and Creative Endeavors Committee for its financial support for this research.

[1] C. S. Wood, S. C. Bennett, D. Cho, B. P. Masterson, J. L. Roberts, C. E. Tanner, and C. E. Wieman, Science **275**, 1759 (1997).
[2] R. J. Rafac, C. E. Tanner, A. E. Livingston, K. W. Kukla, H. G. Berry, and C. A. Kurtz, Phys. Rev. A **50**, R1976 (1994).
[3] L. Young, W. T. Hill III, S. J. Sibener, S. D. Price, C. E. Tanner, C. E. Wieman, and S. R. Leone, Phys. Rev. A **50**, 2174 (1994).
[4] B. Hoeling, J. R. Yeh, T. Takekoshi, and R. J. Knize, Opt. Lett. **21**, 74 (1996).
[5] V. A. Dzuba (private communication).
[6] K. Kiemax, J. Quant. Spectrosc. Radiat. Transf. **17**, 125 (1977).
[7] M. Fabry, J. Quant. Spectrosc. Radiat. Transf. **16**, 127 (1976).
[8] W. H. Press, S. A. Teukolsky, W. T. Vetterling, and B. P. Flannery, *Numerical Recipes in FORTRAN* (Cambridge University Press, Cambridge, 1992).
[9] M. A. Bouchiat, J. Guéna, P. Jacquier, and M. Lintz, Z. Phys. D **24**, 335 (1992).
[10] J. Marek, J. Phys. B **10**, L325 (1977).
[11] A. Sasso, W. Demtröder, T. Colbert, C. Wang, E. Ehrlacher, and J. Huennekens, Phys. Rev. A **45**, 1670 (1992).
[12] H. Lundberg and S. Svanberg, Phys. Lett. **56A**, 31 (1976).
[13] J. S. Deech, R. Luypaert, L. R. Pendrill, and G. W. Series, J. Phys. B **10**, L137 (1977).
[14] W. S. Neil and J. B. Atkinson, J. Phys. B **17**, 693 (1984).
[15] C. E. Theodosiou, Phys. Rev. A **30**, 2881 (1984).
[16] O. S. Heavens, J. Opt. Soc. Am. **51**, 1058 (1961).
[17] P. M. Stone, Phys. Rev. **127**, 1151 (1962).
[18] B. Warner, Mon. Not. R. Astron. Soc. **139**, 115 (1968).
[19] C. E. Moore, *Atomic Energy Levels*, Natl. Bur. Stand. (U.S.) Circ. No. 467 (U.S. GPO, Washington, DC, 1958), Vol. 3.
[20] J. C. Weisheit, Phys. Rev. A **5**, 1621 (1972).
[21] V. A. Dzuba, V. V. Flambaum, A. Ya. Kraftmakher, and O. P. Sushkov, Phys. Rev. A **142**, 373 (1989).
[22] V. A. Dzuba, V. V. Flambaum, and O. P. Sushkov, J. Phys. B **17**, 1953 (1984).
[23] Wo Yei, A. Sieradzan, E. Cerasuolo, and M. D. Havey, Phys. Rev. A **57**, 3419 (1998).